Brodogradnja Volume 75, Number 3 (2024) 75302

journal homepage: www.brodogradnja.fsb.hr

Brodogradnja

An International Journal of Naval Architecture and Ocean Engineering for Research and Development

Research on temperature distribution in container ship with Type-B LNG fuel tank based on CFD and analytical method

Jinfeng Liu[1,2], Guoqing Feng[1], Jiaying Wang[2] , Tianwei Wu[2] , Chen Xu[1] and Kai Yang[1,3]*

[1] *College of Shipbuilding Engineering, Harbin Engineering University, Harbin 150001, China*

[2] *Hudong-Zhonghua Shipbuilding (Group) CO., Ltd., Shanghai 200129, China*

[3] *China Classification Society Harbin Branch, Harbin 150070, China*

ARTICLE INFO

Editor-in-Chief: Prof. Nastia Degiuli

Associate Editor: PhD Ivana Martić

Keywords:

Type-B LNG fuel tank

CFD method

Analytical method

Temperature field

Parametric analysis

ABSTRACT

The liquefied natural gas (LNG) fuel tank in a large container ship is loaded with liquid LNG at an ultra-low temperature (-163°C), there is a significant temperature difference in the cargo hold area where the entire fuel tank is located, which will have an important impact on the steel grade design and structural safety of the cargo tank in container ship. This paper develops two heat transfer models using Computational Fluid Dynamics method (CFD method) and an analytical method to analyze the temperature distribution in a large container ship equipped with Type-B LNG fuel tank. These models incorporate the arrangement and heat transfer characteristics of LNG fuel tanks. The temperature field analysis is conducted under typical the environmental conditions specified in the Code for the Construction and Equipment of Ships Transporting Liquefied Gas in Bulk (IGC Code) and the United States Coast Guard Code (USCG Code), based on the CFD method and the analytical method, and the results of temperature field distribution are compared. Additionally, a parametric analysis of the hull temperature field is further carried out, the results show that the thermal conductivity of the insulation layer in LNG storage tanks and the types of the loaded liquid cargo have a limited impact on the final temperature field distribution in hull structure. However, the selection of steel grade in the local structure of the cargo hold, especially in the inner hull part, may lead to significant changes.

1. Introduction

As the world economy grows faster than ever before, the strong demand for international trade leads to an increase in the size of shipping vessels. Over the years, the presence of ultra-large container ships on major liner routes worldwide has been steadily and significant growing. Simultaneously, in the response to the International Maritime Organization's (IMO) stringent regulations regarding nitrogen oxide and sulfur oxides emissions from ships [1], the adoption of liquefied natural gas (LNG) as fuel has emerged as a trend that benefits for emissions reduction and cost-efficiency [2-3].

* Corresponding author.

E-mail address: fengguoqing@hrbeu.edu.cn

http://dx.doi.org/10.21278/brod75302

Submitted 06 January 2024; Accepted 04 April 2024

ISSN 0007-215X; eISSN 1845-5859

For the ships which use LNG as fuel, the LNG tank is the main feature which stores the LNG at an ultra-low temperature. The Type-B LNG fuel tank, recognized as an independent liquid tank, is recommended by international codes due to its high rate of capacity utilization. The internal design of Type-B LNG fuel tank is effective to mitigate sloshing problem, in particular, it has great advantages in the LNG fuel tank of large container ships with high requirements for its high rate of capacity utilization and anti-sloshing performance [4-5]. Due to the significant temperature difference between tank and external environment, the heat transfer always occurs among the external environment, cargo tank and liquid cargo containment system. The heat transfer will lead to the evaporation rate of the cargo tank, which further affects the selection and the design of liquid cargo system equipment. Moreover, the heat transfer will affect the hull steel grade, which have a great impact on the safety of the entire cargo structure. Therefore, the temperature field analysis is necessary for the safety of ship hull.

Currently, the temperature field analysis mainly adopts the analytical method and the finite element method for LNG carriers. Zhang [6] analyzed the steady-state temperature field of the liquid cargo tank in a 13,8000 m3 LNG carrier, and studied the effects of air convection and surface radiation heat transfer between the outer shell and inner hull. Zhou [7] further to discuss the influence of heat conduction, heat convection and heat radiation on heat transfer in the closed space in membrane LNG carriers. Ding [8] studied the analytical calculation method of heat transfer in the enclosed space of LNG carrier, and based on the analytical method, an equivalent coupling convection coefficient is proposed to simulate the heat transfer between outer and inner hull, the accuracy of the method is verified by comparing the calculation results with the experimental results of Gaztransport & Technigaz (GTT) in France. Wu [9] discussed several issues such as model simplification and assumption during the analysis of the temperature field in membrane LNG carriers, and the influence of thermal conductivity of the insulation layer in secondary barrier were studied. At the same time, it's further to carry out the parametric analysis of the temperature field for membrane LNG carries. Lv [10] also used the analytical method, and carried out relevant research on the temperature field analysis in longitudinal double-shell structure of membrane LNG carriers, and summarized the simplified method for the temperature field analysis of the cargo hold in membrane LNG carriers, but the prediction accuracy of the temperature field needs to be further verified. Lu [11] presents a numerical prediction of the thermodynamics associated with the pre-cooling operation of the membrane-type tanks of the LNG carriers. The results and conclusions may help guiding the temperature distribution in pre-cooling operation for LNG carriers.

In summary, the above studies have carried out a lot of research work on the temperature field analysis of large LNG carriers, especially for membrane LNG carriers. There the analytical method usually decomposes the cargo hold into different hull areas, and then one-dimensional heat transfer calculations are then used for each area [12]. Although the temperature of the hull structure at a specific location can be quickly obtained by this method, the calculation results are often conservative because the heat transfer process between different regions cannot be considered. The finite element method can obtain the temperature distribution of each position in the cargo hold area, but because the method cannot calculate convective heat transfer and radiation heat transfer well, the final calculation result is greatly affected by the input comprehensive heat transfer coefficient, and which is often obtained based on the analytical method. Therefore, when convective heat transfer and radiative heat transfer have a great influence on the temperature field calculation, this method has specific limitations, and the results are often close to the analytical method. Compared with the previous membrane LNG carriers, the arrangement design of the Type-B LNG fuel tank in container ship studied in this paper is very different, and there is a cargo hold space between the liquid cargo tank and inner hull structure, which is free-flowing, and the heat transfer process is mainly dominated by convective heat transfer and radiation heat transfer, and it may be difficult to obtain the accurate temperature field results in the above space, if the analytical method and the finite element method are used.

Li [13] established the heat transfer model and evaporation rate calculation of new LNG ship liquid cargo insulation system, and carried out the research for temperature distribution of cargo tank. Wu [14-15] simulated the two-phase flow and phase change heat transfer of a cryogenic fluid in the Type-B mock up tank, by unsteady three-dimensional computational fluid dynamics (CFD) method, and the numerical simulation and experiment verification of the static boil-off rate and temperature field was studied in relevant references.

However, the above research is limited to the Type-B mock up tank, and there is no relevant research on the Type-B LNG fuel tank in container ship, and there is a lack of comparative research on CFD methods and analytical methods. Niu [16] discussed a new thermal insulation system for cargo containment system (CCS) in LNG carriers, and the conductivities of the insulation materials were tested and the heat transfer model of this carrier was established and simulated, in order to quantitatively evaluate the thermal insulation performance, which provides ideas for the study in the temperature distribution of Type-B LNG fuel tanks in this paper.

Therefore, this paper synthesizes the research results of relevant references, taking the Type-B LNG fuel tank in container ship independently developed and designed by a shipyard as the research object, and focuses on the study of heat transfer mechanism and simulation calculation method for the Type-B LNG liquid cargo tank. And the CFD method and the analytical method are used in the temperature field calculation in the cargo hold area, respectively, based on the environmental conditions specified in the Code for the Construction and Equipment of Ships Transporting Liquefied Gas in Bulk [17] (IGC Code) and the United States Coast Guard Code [18] (USCG Code). Meanwhile, the difference between the above temperature field calculation methods was further discussed. Finally, the influence of the insulation conductivity and the types of liquid cargo on the structural temperature distribution has been deeply studied.

2. Heat transfer analysis mechanism and calculation conditions

2.1 Target LNG fuel tank and heat transfer model

In present study, a container ship power by LNG is used for heat transfer analysis, and the arrangement of cargo hold and LNG fuel tank are shown in Figure 1. The low-temperature cold source is liquid LNG loaded in the cargo tank, which is -163°C, and the heat source is outside air and seawater.

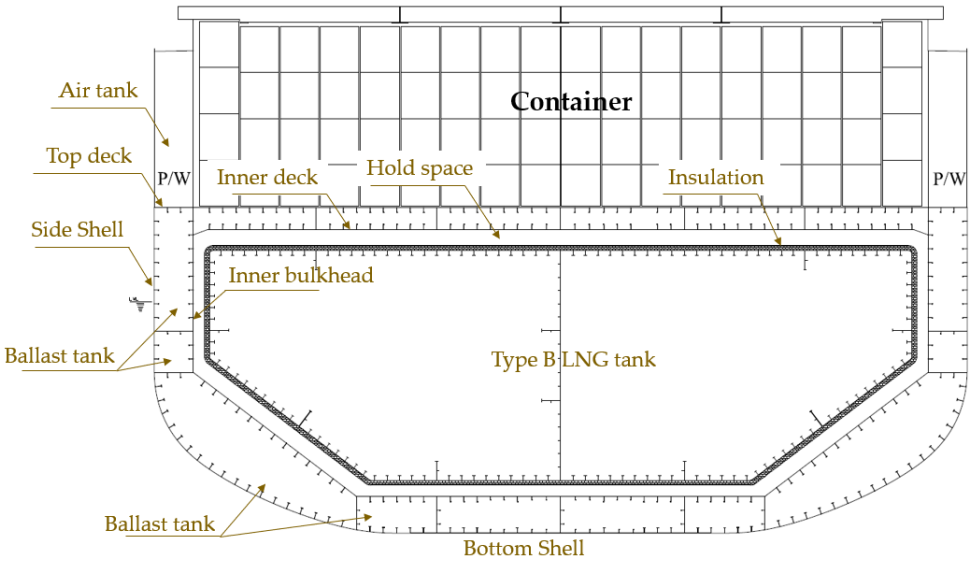

Fig. 1 The arrangement of cargo hold and LNG fuel tank in container ship.

Since the structure of ship hull and LNG tank are symmetric, the analysis and investigation are focused on the left part of the hull and tank to simplify the computational process. The simplified model and the process of heat transfer are shown in Figure 2. The heat transfer mainly includes the 5 steps: (1) Heat transfer through air or seawater to outer shell by convective heat exchange; (2) Heat transfer through outer shell transfers heat to the ballast tank space by large space convection heat transfer and space radiation heat exchange; (3) Heat transfer through ballast tank space to the inner hull by convective heat exchange and space radiation heat exchange; (4) Heat transfer through inner hull to the outer surface of the insulation layer by convective heat exchange and radiant heat exchange; (5) Heat transfer through the insulation to fuel tank by heat conduction.

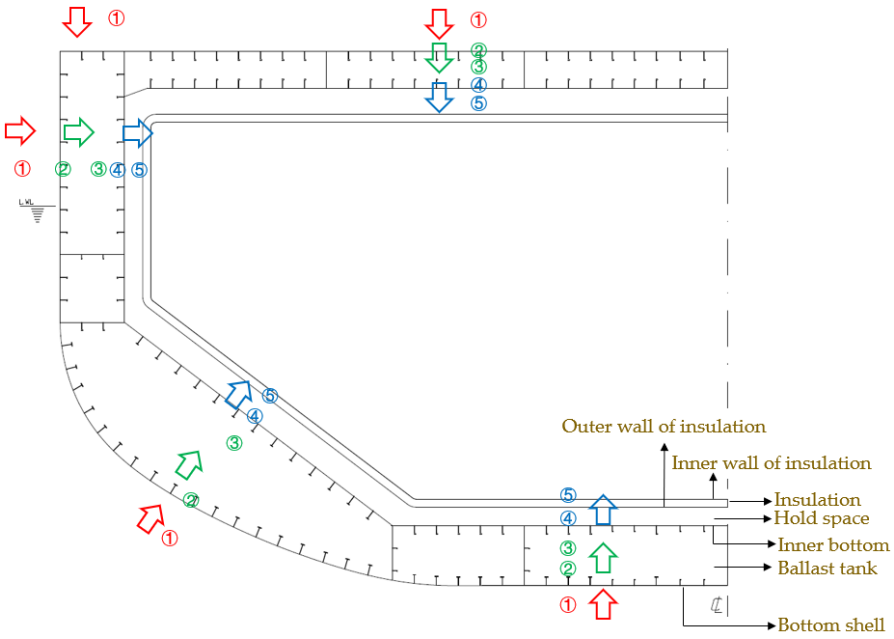

Fig. 2 The overall heat transfer model of the cargo hold.

2.2 Environmental conditions and material properties

Table 1 presents the external environmental conditions specified by IGC and USCG for analyzing the temperature field in the cargo compartment, and the material properties of hull structural steel and insulation are shown in Table 2.

Table 1 External environmental conditions

	IGC Conditions	USCG conditions
Air temperature(°C)	5	–18
Sea water temperature(°C)	0	0
Wind speed (kn)	0	5

Table 2 Material properties

	Insulation	Structural steel
Density(kg/m^3)	27	8030
Specific heat capacity(J/(kg·°C))	1100	502.48
Thermal conductivity (W/(m·K)).	0.024	16.27

The numbers of cargo division compartments and structural plates are shown in Figure 3. The following assumptions are listed:

(1) The heat transfer process is assumed as a steady process;

(2) The inner side of the insulation is in direct contact with LNG, maintaining a constant temperature of –163°C;

(3) The ballast tank contains air, whereas the cargo hold space contains nitrogen; both are treated as ideal gases with no exchange among themselves or with the external environment.

(4) The steel of hull structure is assumed to have uniform thermal conductivity, with unchanging physical properties across temperature variations. The thermal conductivity in the direction of hull's thickness is disregarded, and the temperature is considered consistent on both the interior

and exterior of the hull.

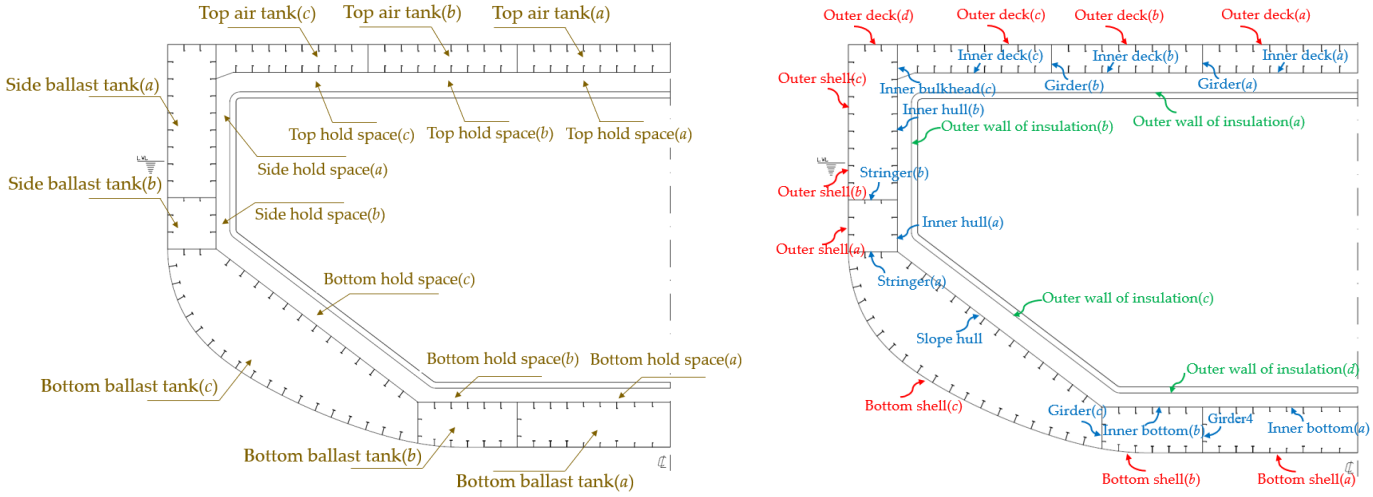

(a) Definition of heat transfer space (b) Wall definition

Fig. 3 Definition of each space and wall in the target cargo hold.

Based on the above heat transfer model and temperature boundary, the CFD method and analytical method were used to analyze the structural temperature field, respectively.

3. Mathematical model

3.1 CFD calculation model

As previously analyzed, the heat transfer process of Type-B LNG fuel tank includes heat conduction, convective heat transfer and radiation. Fluid medium flow is also involved in the ballast tank and cargo compartment space area. According to the heat transfer characteristics, the following CFD calculation model is established:

(1) Continuity equation:

$$\frac{\partial(\rho u)}{\partial x}+\frac{\partial(\rho v)}{\partial y}=0 \tag{1}$$

where, ρ is the fluid density, kg/m^3, u and v are the fluid velocity in the direction x, y respectively, m/s.

(2) Momentum conservation equation:

$$\nabla\cdot(\rho vv)=-\nabla p+\nabla\cdot\left(\mu(\nabla v+\nabla v^T)\right)+\rho g+F \tag{2}$$

where, v is the fluid velocity; p is the pressure, Pa; μ is dynamic viscosity, Pa·s; F is the volumetric force acting on the control bodies, N.

(3) Energy conservation equation:

$$\nabla\cdot\left(v(\rho E+p)\right)=\nabla\cdot\left(k_{eff}\nabla T\right)+S_h, \tag{3}$$

where, S_h is the volumetric heat source term, (kg·W) /m^3; k_{eff} is the effective thermal conductivity; T is the temperature, K; E is energy, J.

(4) RNG turbulence model:

$$\frac{\partial(\rho k u_i)}{\partial x_i}=\frac{\partial}{\partial x_j}\left(\alpha_k\mu_{eff}\frac{\partial k}{\partial x_j}\right)+G_k+G_b-\rho\varepsilon-Y_M+S_k, \tag{4}$$

$$\frac{\partial(\rho\varepsilon u_i)}{\partial x_i}=\frac{\partial}{\partial x_j}\left(\alpha_\varepsilon\mu_{eff}\frac{\partial\varepsilon}{\partial x_j}\right)+C_{1\varepsilon}\frac{\varepsilon}{k}(G_k+C_{3\varepsilon}G_b)-C_{2\varepsilon}\rho\frac{\varepsilon^2}{k}-R_\varepsilon+S_\varepsilon, \tag{5}$$

where, G_b is the turbulent kinetic energy term caused by buoyancy; G_k is the turbulent kinetic energy term caused by the average velocity gradient; Y_M is the dissipation term caused by compressible turbulent pulsation

expansion; μ_{eff} is the effective viscosity; R_ε is the additional term in the dissipation equation; α_k and α_ε are turbulent kinetic energy and dissipation rate coefficients, respectively; S_k *and* S_ε are the source terms of turbulent kinetic energy and dissipation rate; $C_{1\varepsilon}$,$C_{2\varepsilon}$ and $C_{3\varepsilon}$ are constants.

(5) DO radiation model:

$$\nabla \cdot (I(\vec{r},\vec{s})\vec{s}) + (a+\sigma_s)I(\vec{r},\vec{s}) = an^2\frac{\sigma T^4}{\pi} + \frac{\sigma_s}{4\pi}\int_0^{4\pi} I(\vec{r},\vec{s}')\,\Phi(\vec{s}\cdot\vec{s}')d\Omega' \tag{6}$$

where, $\vec{r}$ is the position vector; $\vec{s}$ is direction vector; $\vec{s}'$ is the scattering direction vector, a absorption rate in wall; n is the wall refractive index; σ_s is the scattering coefficient; and σ is the Stephen-Boltzmann constant, which is 5.67×10^{-8} W/(m^2·K^4); I is the radiant intensity; T is the temperature; Φ is the phase function; and Ω' is the angle.

In the calculational process, the heat transfer coefficient and fluid temperature on the outer shell plate are given which is the third-type of thermal boundary conditions. The temperature on the inner sider of the insulation is given which satisfy the first type of the thermal boundary conditions. The control equation is solved by the temperature field calculation model which is based on the steady pressure state solver. The pressure and velocity are calculated by coupled algorithm. The pressure, momentum, and energy are calculated by the second-order windward term. The number of CFD mesh is about 31,000 for this cargo temperature field analysis.

3.2 Analytical method

Compared with the CFD method, the analytical method has been simplified in heat transfer model for cargo hold tank. As an example, Figure 4 presents a simplified one-dimensional heat transfer model in side area of cargo hold, based on the analytical method, where q_1 is the heat exchange between air/sea water and the outer plate of the ship. q_2 is the heat exchange between the outer plate and the ballast tank space; q_3 is the heat exchange between the ballast tank space and the inner hull; q_4 is the heat exchange between the inner hull and the outer wall of the insulation; q_5 is the heat exchange between the outer wall of the insulation and the inner wall of the insulation; Based on the theory of thermal equilibrium, the following equations can be obtained:

$$q_1 = q_2 = q_3 = q_4 = q_5 \tag{7}$$

These parameters can be calculated by:

$$q_1 = h_{con}^1(T_0 - T_1) \tag{8}$$

$$q_2 = (h_{con}^2 + h_{rad}^1)(T_1 - T_M) \tag{9}$$

$$q_3 = (h_{con}^3 + h_{rad}^2)(T_M - T_2) \tag{10}$$

$$q_4 = (h'_{con} + h'_{rad})(T_2 - T_3) \tag{11}$$

$$q_5 = \frac{\lambda(T_3 - T_{LNG})}{\delta} \tag{12}$$

In the above formula, $q_1 \sim q_5$ are the heat transfer of each process; T_0 is the external ambient temperature(air or seawater), T_1 is the temperature at outer shell, T_0 is the external ambient temperature(air or seawater), T_2 is the temperature at inner hull, T_{M} is the temperature in compartment between the outer shell and the inner hull, T_3 is the temperature at outer wall in insulation, T_{LNG} is the liquid temperature inside LNG fuel tank; h_{con}^1, $h_{con}^1$and h_{con}^1 are the convective heat transfer coefficient of large space plates; h'_{con} is the convective heat transfer coefficient of limited space; h_{rad} is the radiative equivalent convective heat transfer coefficient; δ is the thickness of the insulation; λ is the thermal conductivity of the insulation.

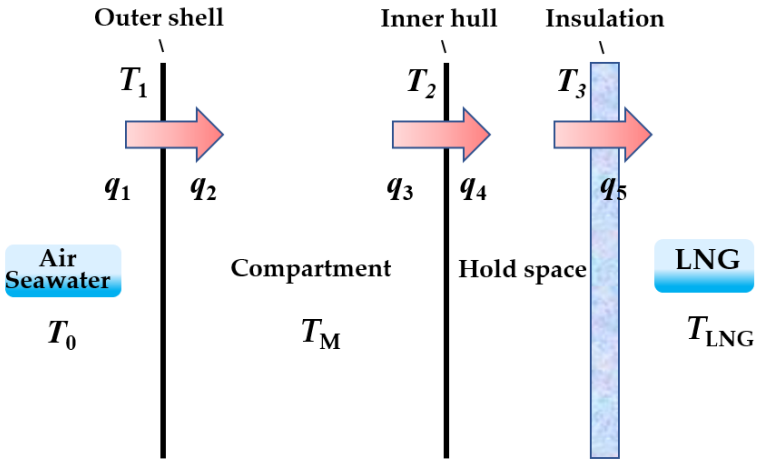

Fig. 4 One-dimensional heat transfer model simplified by analytical method

For the flat plate structure with large space, the convective heat transfer coefficient can be expressed as the formula (13). The convective heat transfer coefficient between the outer shell and the external environment/compartment, and between the inner shell and the compartment are obtained based on the calculation formula (13) for large space flat plate[19].

$$h = C\frac{l}{\lambda}(Gr \cdot Pr)^n, \tag{13}$$

where, l is the spatial characteristic length; λ is the thermal conductivity of the fluid; Gr is the Grachev number, $Gr = \frac{g\beta x^3 \Delta T}{\nu^2}$, ΔT is the temperature difference between fluid and wall, β is the thermal expansion coefficient, x is the geometric feature length, ν is the kinematic viscosity of fluids, Pr is the Plantl number, C and n are constants, and the values of C and n in different location and condition are shown in the following Table 3, in the case of inclined plates, the convective heat transfer refers to the vertical plates, and depends only on the angle of the inclined plates.

Table 3 Convective heat transfer coefficient of large space flat plate

Heat exchange surface		C	n	Restrictions
The vertical flat plate/ The inclined plate		0.59	1/4	$1.43\times10^4<Gr\leq3\times10^9$
		0.0292	0.39	$3\times10^9<Gr\leq2\times10^{10}$
		0.11	1/3	$Gr>2\times10^{10}$
The horizontal flat plate	up	0.54	1/4	$10^5<Gr\leq2\times10^7$
		0.15	1/3	$2\times10^7<Gr\leq3\times10^{10}$
	down	0.27	1/4	$3\times10^5<Gr<3\times10^{10}$

For localized limited space, the convective heat transfer coefficient can be expressed as follows formula [14]. The convective heat transfer coefficient between the inner hull and the outer wall in insulation, are obtained based on the calculation formula (14).

$$h = C\frac{l}{\lambda}(Gr \cdot Pr)^n \left(\frac{H}{\delta}\right)^m \tag{14}$$

where H is the length of the compartment; δ is the thickness of the compartment; n and m under different location and condition are shown in the following Table 4.

Table 4 Convective heat transfer coefficient in localized limited space

Heat exchange surface	C	n	m	Restrictions
Vertical direction	0.197	1/4	-1/9	$8.6\times10^3\leq Gr\leq2.9\times10^5$
	0.073	1/3	-1/9	$2.9\times10^5\leq Gr\leq1.6\times10^7$
Horizontal direction	0.212	1/4	0	$1.0\times10^4\leq Gr\leq4.6\times10^5$
	0.061	1/3	0	$Gr>4.6\times10^5$

For equivalent radiation heat transfer, the convective heat transfer coefficient can be expressed as follows:

$$h=\frac{\varepsilon\sigma(T_1^4-T_2^4)}{T_1-T_2} \tag{15}$$

where the ε is surface emissivity; σ is the constant; T_1, T_2 is the structural wall temperature, respectively.

The specific temperature field calculation process is shown in Figure 5.

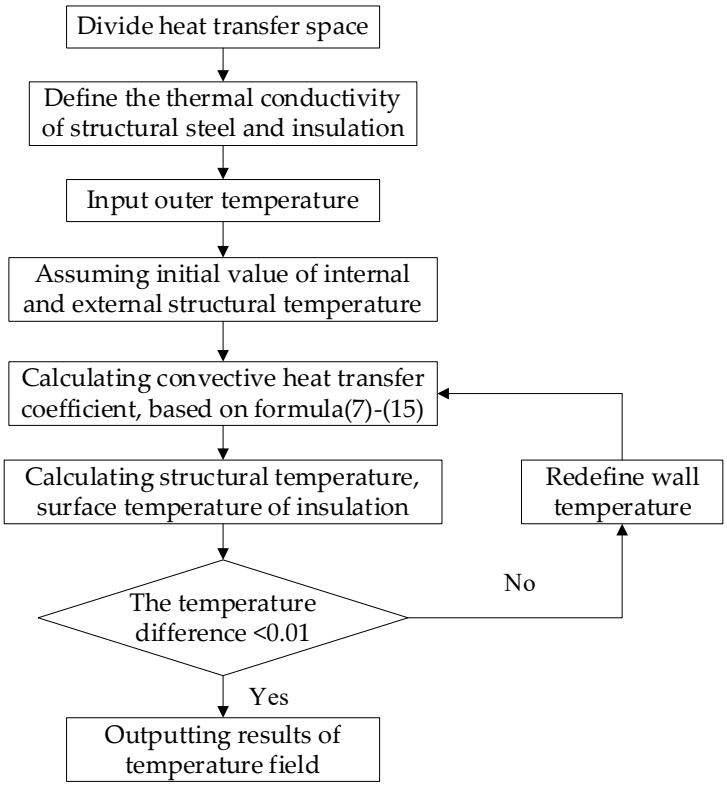

Fig. 5 The specific temperature field calculation process

4. Comparison of temperature field distribution based on CFD and analytical method

4.1 Analysis of ballast tank and cargo space temperature field

The temperature field under IGC and USCG conditions is calculated by CFD method. The spatial temperature distribution results of ballast tank and cargo space are shown in Figure 6 and Figure 7, respectively. In IGC condition, the air temperature being higher at 5℃ compared to the sea temperature at 0℃ leads to a gradual temperature decrease in the cargo hold area, progressing from the top and bottom. It is concluded that heat from the upper air is transferred to the area below the waterline. This heat transfer occurs through the vertical flow of gases in the air tank or the cargo hold space, within the vertical direction of the cargo hold. It can also be seen that the lowest spatial temperature is observed at the bottom ballast tank (*a*).

This is caused by the larger size of the bottom ballast compartment compared to other areas and its greater distance from external heat sources, so the heat exchange in this area is relatively lower .

In USCG conditions, as the sea temperature being higher at 0℃ compared to the sea temperature at –18℃, the temperature in cargo hold is gradually increase from top to bottom. And the heat from the seawater is transferred to the area above the waterline via the vertical gas flow within the ballast tank and cargo space of the cargo hold. The lowest spatial temperature is observed in the top air tank (top air space and corresponding top cargo space (*c*)).

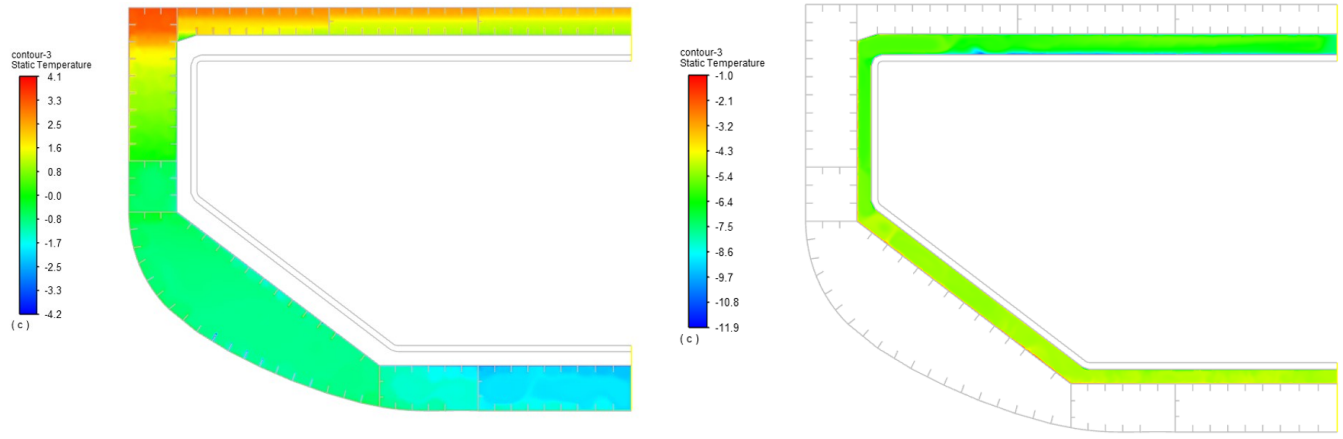

(a) temperature field distribution in ballast tank (b) Temperature field distribution in cargo space

Fig. 6. Calculation results of cargo compartment area temperature based on CFD method (IGC Condition)

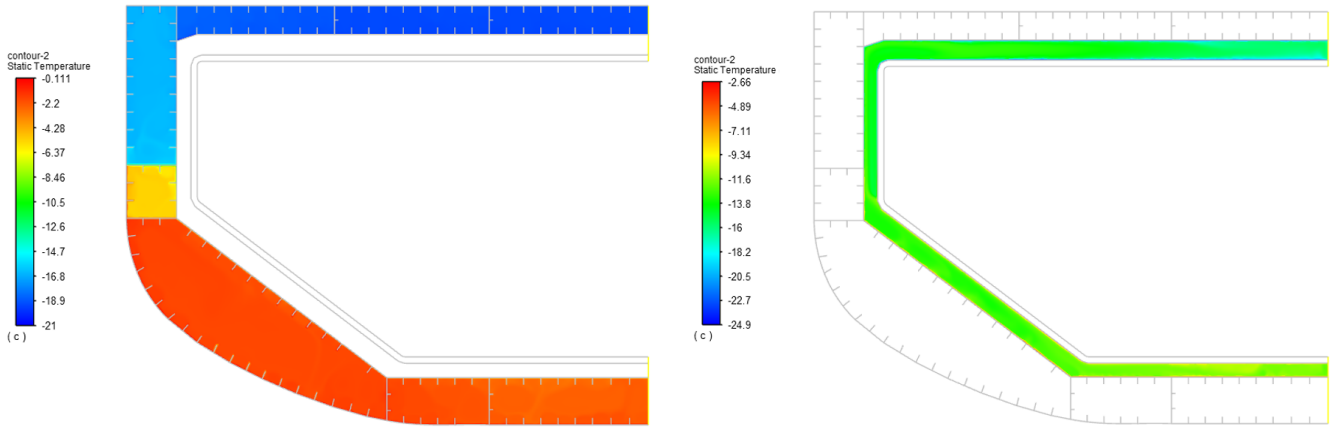

(a) temperature field distribution in ballast tank (b) Temperature field distribution in cargo space

Fig. 7 Calculation results of cargo compartment area temperature based on CFD method (USCG conditions)

Table 5 presents the space temperature results for each tank space, calculated by CFD method and analytical method. For the ballast tank area under the waterline, the results obtained by CFD method and analytical method exhibit minimal differences. While, for the empty deck tank in the top, the results obtained by analytical method are higher than those obtained by CFD method, and significant differences are observed. Table 6 shows the temperature of the cargo hold space, as predicted by two different methods. It can be seen that under the IGC condition, two methods can provide similar results. For the spatial temperature in USCG conditions, a significant difference is observed between the results obtained by two methods, the temperature results obtained using CFD method are higher than those from the analytical method above the waterline, yet lower below the waterline. Generally, the temperature distribution as calculated by the CFD method exhibits relative uniformity.

When employing CFD method, the spatial area of the cargo hold is configured as a vertically connected space. Within this space, the convection effect of gas facilitates the transfer of heat from below the waterline

(or the cold energy in the space above the waterline) to the opposite side. As shown in Figure 8(b), the temperature distribution of the entire cargo space is relatively uniform.

In the application of the analytical method, the spatial area of the cargo hold is divided into isolated spaces. This segmentation hinders the heat transfer between these spaces, leading to higher temperature below the waterline and lower temperature above the waterline.

As shown in Figure 8(a), due to the slight temperature different between air and sea, the convection effect is weak in IGC condition. This leads to minimal heat transfer within the cargo space, resulting in negligible differences between the results obtained by these two methods.

Table 5 Temperature results of each tank space obtained by CFD method and analytical method

Cargo hold location		IGC condition		USCG	
		CFD method	Analysis method	CFD method	Analysis method
Top air tank	(a)	1.6℃	–0.8℃	–16.2℃	–20.6℃
	(b)	1.7℃	–0.8℃	–16.2℃	–20.6℃
	(c)	2.1℃	–0.8℃	–16.3℃	–20.6℃
Side ballast tanks	(a)	1.4℃	0.6℃	–15.9℃	–18.2℃
	(b)	–0.7℃	–0.3℃	–5.3℃	–3.0℃
	(c)	–2.3℃	–0.4℃	–3.2℃	–0.4℃
Bottom ballast tank	(a)	–1.4℃	–1.6℃	–2.0℃	–1.6℃
	(b)	–1.9℃	–1.6℃	–2.6℃	–1.6℃

Table 6 Temperature results of each cargo space obtained by CFD method and analytical method

Cargo hold location		IGC		USCG	
		CFD method	Analysis method	CFD method	Analysis method
Top cargo hold space	(a)	–6.4℃	–4.5℃	–13.6℃	–22.9℃
	(b)	–6.0℃	–4.3℃	–14.3℃	–22.9℃
	(c)	–5.5℃	–3.9℃	–13.9℃	–22.9℃
Side cargo hold space	(a)	–6.0℃	–4.2℃	–13.0℃	–20.7℃
	(b)	–6.3℃	–4.6℃	–12.7℃	–4.6℃
	(c)	–6.7℃	–4.4℃	–12.8℃	–4.4℃
Bottom cargo hold space	(a)	–5.0℃	–4.1℃	–12.1℃	–4.1℃
	(b)	–4.7℃	–4.1℃	–11.8℃	–4.1℃

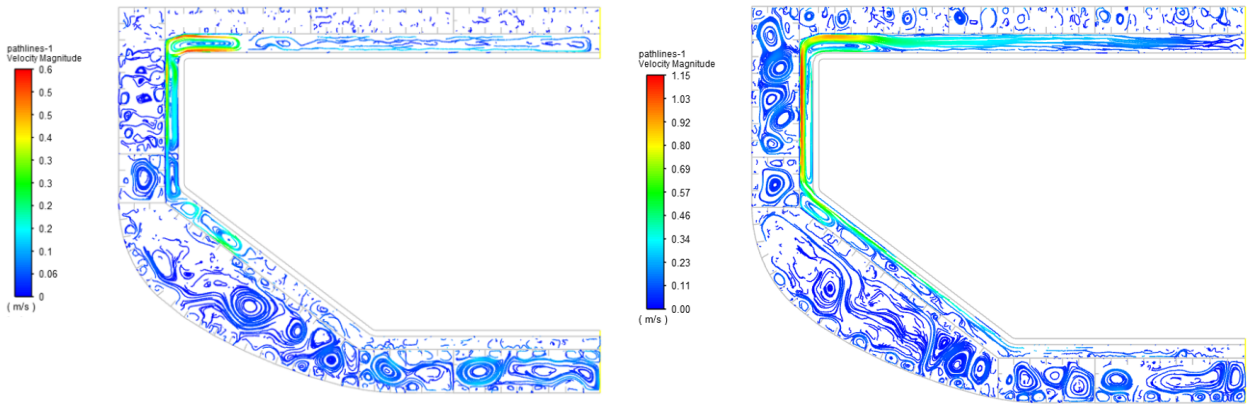

(a) IGC condition (b) USCG condition

Fig. 8 The results of flow field.

4.2 Temperature field analysis of hull structure and insulation

Figure 9 shows the temperature results for the hull structure and outer wall of insulation, as obtained by the CFD method in IGC condition. As can be seen from Figure 9(a), the lowest temperature is observed in the slope hull, while in USCG condition, the lowest temperature occurs on the top inner deck (b), which can be seen from Figure 9(b).

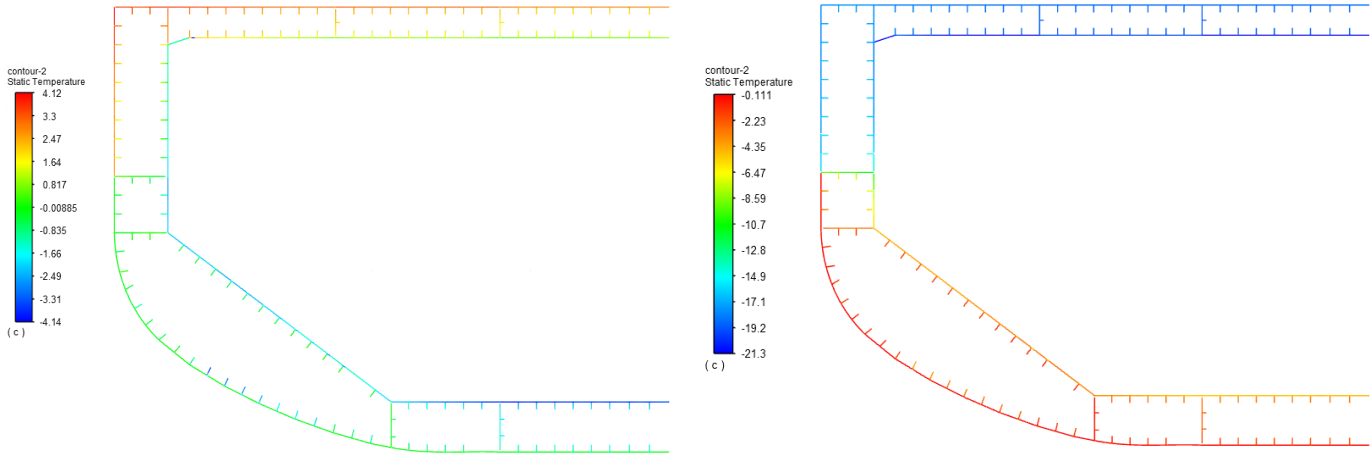

(a) IGC Condition (b) USCG condition

Fig. 9 Temperature results of hull structure and outer wall of insulation based on CFD method

Table 7 presents a comparative analysis of the temperature fields results for the hull structure and the outer wall of the insulation, as predicted using both CFD method and the analytical method. As shown in Table 7, due to the limited heat transfer between the local space above and below the waterline in IGC condition, the difference between the results obtained by these two methods is slight.

But under USCG condition, a notable discrepancy between the results obtained from these two methods is presented. It is particularly evident in the inner hull and outer wall of insulation, encompassing the inner hull (a), inner hull (b), and the outer wall of the insulation (b) near the waterline. Under the USCG condition, the sea water temperature is much lower than the air temperature, and strong convective heat transfer will occur near the waterline. Therefore, the results differ greatly from the analytical method calculated separately for each region.

It can be seen that the temperature of the hull structure calculated by CFD method is higher, compared to the results from the analytical method, this discrepancy is attributed to the lowest temperature occurrence in the hull structure, which is located in the inner hull area. The structural steel grade in this area is established

based on the USCG environmental conditions. Therefore, the steel grade selected based on the results of analytical method tends to be more conservative, compared to those derived from the CFD method.

Table 7 Temperature field in hull structure and outer wall of insulation under CFD method and analytical method

Location		IGC condition		USCG condition	
		CFD method	Analysis method	CFD method	Analysis method
Outer deck	(a)	2.9℃	2.7℃	–18.6℃	–20.6℃
	(b)	3.3℃	3.0℃	–18.6℃	–20.5℃
	(c)	3.3℃	3.1℃	–18.3℃	–20.2℃
	(d)	3.6℃	3.4℃	–17.5℃	–19.4℃
Bottom shell	(a)	–0.1℃	–0.1℃	–0.2℃	–0.1℃
	(b)	–0.1℃	–0.1℃	–0.2℃	–0.1℃
	(c)	–0.1℃	–0.1℃	–0.3℃	–0.1℃
Outer shell	(a)	–0.1℃	–1.1℃	–0.4℃	–1.1℃
	(b)	2.7℃	2.6℃	–16.4℃	–18.4℃
	(c)	3.2℃	2.3℃	–17.6℃	–19.5℃
Inner deck	(a)	0.6℃	1.8℃	–21.1℃	–25.5℃
	(b)	0.8℃	1.8℃	–21.1℃	–25.5℃
	(c)	1.0℃	1.8℃	–21.0℃	–25.5℃
Inner bottom	(a)	–3.6℃	–4.1℃	–5.1℃	–4.1℃
	(b)	–3.0℃	–4.1℃	–4.7℃	–4.1℃
Slope hull		–4.1℃	–5.6℃	–6.3℃	–5.6℃
Inner hull	(a)	–2.5℃	–5.2℃	–7.5℃	–5.2℃
	(b)	–1.5℃	–3.0℃	–16.8℃	–21.9℃
	(c)	3.0℃	*	–17.7℃	*
Stringer	(a)	–0.2℃	*	–6.9℃	*
	(b)	0.1℃	*	–1.7℃	*
Girder	(a)	1.8℃	*	–20.3℃	*
	(b)	2.0℃	*	–20.1℃	*
	(c)	–0.2℃	*	–0.9℃	*
	(d)	–1.6℃	*	–2.5℃	*
Outer wall in insulation	(a)	–8.0℃	–9.2℃	–23.2℃	–24.1℃
	(b)	–7.2℃	–7.6℃	–12.5℃	–18.2℃
	(c)	–6.5℃	–5.1℃	–11.3℃	–5.1℃
	(d)	–5.3℃	–4.9℃	–11.0℃	–4.9℃

Note: The hull structure marked by * is an internal component and cannot be solved by analytical method.

Comparing the calculation results of the analytical method under the waterline in Table 5 ~Table 7, it can be seen that the calculation results below the waterline are the same under IGC and USCG conditions. It's a known fact that when using the analytical method to calculate the temperature field, each region in cargo hold is considered separately, ignoring the heat transfer effects between the different regions. Specifically, in

the area below the waterline, the internal and external boundary conditions remain consistent under both IGC and USCG environmental conditions, which leads to identical calculation results in above regions.

5. Parametric analysis of hull temperature field

5.1 Influence of thermal conductivity on hull temperature distribution and steel selection

To quantitatively analyze the impact of insulation thermal conductivity on the hull temperature distribution and steel grade selection, this study focuses on varying the thermal conductivity of the insulation system alone, with all other parameters remaining constant. The thermal conductivity values considered are 0.01, 0.02, 0.03, 0.04, 0.05, and 0.06. Subsequently, a temperature field analysis will be conducted using the CFD method.

Drawing from design experience, the USGC environmental condition is identified as the prevailing factor in the selection of hull steel grade. This paper specifically examines the effects of changes in the thermal conductivity of insulation system, on the temperature distribution of the inner hull structures in USCG conditions. Figure 10 illustrates the relationship between the thermal conductivity of insulation system and the resultant temperature variations in the inner hull structure of the cargo hold.

Figure 10 reveals that the temperature of the inner hull structure exhibits a gradual decrease as the thermal conductivity of the insulation system increases. However, this reduction is relatively modest. Based on the calculations presented in this study, a 0.01 W/(m·K) increase in the thermal conductivity of insulation system correlates with a temperature decrease of approximately 1.2–2.3 °C in the inner hull.

The analysis indicates that variations in the thermal conductivity of the insulation system exert minimal impact on the distribution of the structural temperature field. As IGC rules[17], changes in the steel plate grade are necessitated when its temperature reaches –5, –10, –20, or –30 °C.

Figure 10 also illustrates that, while variations in the thermal conductivity of insulation system minimally affect the final temperature field distribution, they can still influence the choice of steel grade. For instance, in the case of the inner deck, enhancing the physical properties of insulation material to improve the thermal conductivity of insulation system by over 8%. the thermal conductivity of the insulation system is reduced from 0.024 W/(m·K) to 0.022 W/(m·K), resulting in the downgrading of the steel grade in inner hull from DH to D.

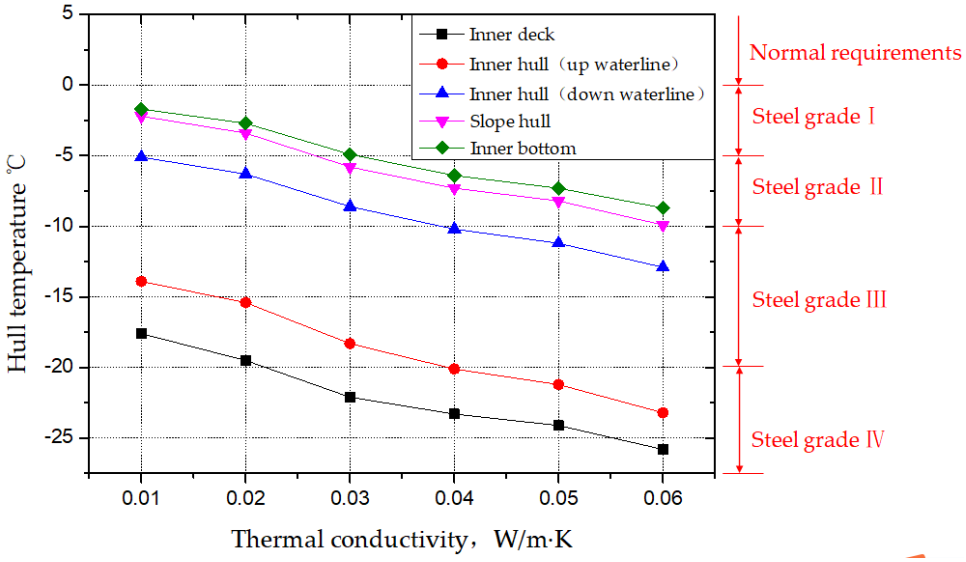

Fig. 10 The temperature calculation result in the inner hull under the different thermal conductivity.

5.2 Influence of liquid cargo temperature on hull temperature distribution and steel selection

With the diversification of petrochemical energy trade, the ethane (–104°C), ethylene (–88°C), liquefied petroleum gas (–42°C), and even liquid ammonia (–33°C) and other liquid cargo with higher temperatures compared to the liquefied natural gas, loading in cargo hold structure. Due to the high temperature of the loaded liquids, the temperature of the structure connected to the insulation system will change accordingly. In this paper, other parameters are unchanged, focusing on the influence of different types of loaded cargo under USCG environmental conditions, that is, the influence of liquid cargo temperature change on the temperature distribution of hull structure. Figure 11 shows the change curve of the temperature calculation result of the inner hull structure in the cargo hold as a function of the temperature in the loaded liquid cargo.

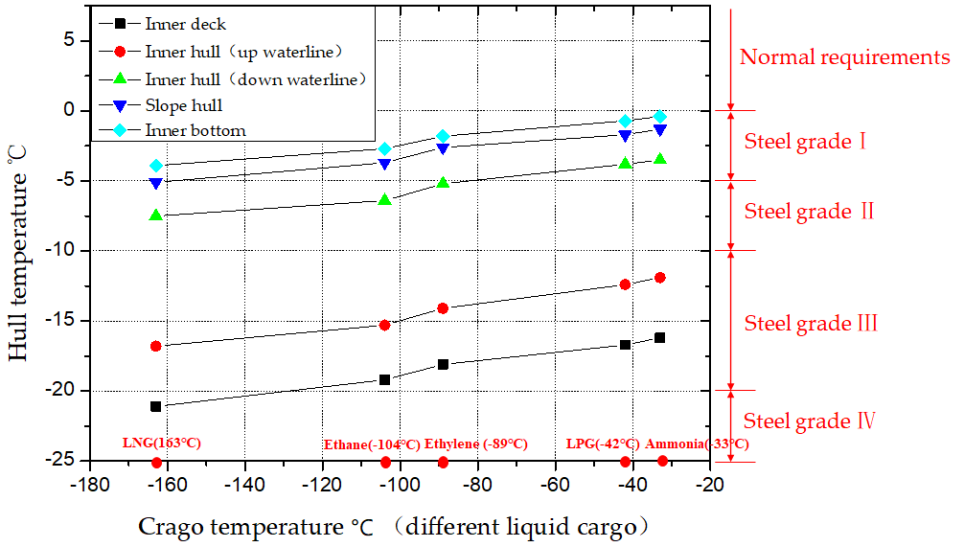

Fig. 11 The temperature calculation result in the inner hull under different types of liquid cargo

Figure 11 illustrates the distinct impacts of various liquid cargo types on the temperature distribution within the inner hull structure of a cargo hold, particularly in USCG conditions. Notably, the internal hull temperature fluctuates minimally, by no more than 5 °C, despite significant variations in liquid cargo temperatures, ranging from –163 °C (LNG) to –33 °C (liquid ammonia). Under USCG environmental conditions, where the external air temperature is –18 °C and seawater temperature is at 0 °C, the heat transfer principles dictate that the structural temperature above the waterline cannot exceed –18 °C, and that below the waterline, it cannot surpass 0 °C. Consequently, the inner hull structure's temperature, in connection with the insulation system, remains relatively stable, even with increasing temperatures of the liquid cargo.

It should be emphasized that the minimum temperature in inner hull falls below –20°C when LNG liquid cargo at –163°C is loaded, necessitating a more stringent steel grade selection. Conversely, when cargoes such as ethane, ethylene, LPG, and liquid ammonia are loaded, the calculated temperature of the inner deck in USCG conditions exceeds –20°C. Consequently, based on the IGC code requirements, it’s permissible to downgrade the steel grade from DH to D. Additionally, as the temperature of the loaded cargo increases, a corresponding downgrade in the steel grade material for the longitudinal inner hull may also be considered.

6. Conclusion

In this paper, a steady-state heat transfer analysis was conducted for the cargo hold in a container ship equipped with a Type-B LNG fuel tank. The temperature field calculations under IGC and USCG environmental conditions were performed using both CFD and analytical methods. This study compares the temperature field distributions derived from these two distinct methods, further investigating the effects of thermal conductivity in insulation and variations in liquid cargo temperature on the structural temperature field distribution and the selection of steel grades. The conclusions drawn are as follows:

1) In IGC conditions, convection and heat exchange effects near the waterline, both above and below, are minimal due to the negligible temperature difference between the outside air and sea. Consequently, the

temperature results obtained via both the CFD and analytical methods are remarkably similar. However, in USCG environmental conditions, the significant disparity between outside air and seawater temperatures leads to pronounced convection and heat transfer effects within the cargo hold space. The CFD method, adept at simulating the comprehensive flow and heat transfer in this space, reveals a marked difference in temperature field distribution compared to results obtained via the analytical method. Consequently, steel grade design based on the temperature field distribution derived from the analytical method tends to be overly conservative.

2) In practical engineering applications, the empirical correlation-based analytical method is relatively simple and expedient, offering distinct advantages for early-stage predictions of structural temperature and steel grade design in liquid cargo ships carrying low-temperature LNG. However, for areas experiencing strong flow effects, such as the cargo space housing the Type-B LNG fuel tank, the analytical method's temperature field analysis exhibits significant limitations, often resulting in considerable deviations. Therefore, for future design and development of vessels with spaces akin to the flowing hold space discussed in this study, temperature field prediction based on the CFD method is more advisable.

3) When the thermal conductivity of the insulation layer increases by 0.01 W/(m·K), the temperature of the inner hull decreases by approximately 1.2–2.3°C. Additionally, even with an increase in the temperature of the liquid cargo, the inner hull structure's temperature does not significantly rise. However, while the selection of insulation's thermal conductivity and the type of loaded liquid cargo have a minimal impact on the final temperature field distribution, these factors can still influence the choice of steel grade, particularly for the inner hull.

4) The heat transfer process within LNG fuel tank cargo tanks is complex. Despite extensive comparative research on the heat transfer calculations of liquid cargo tanks, simplifications are often made in actual engineering calculations to enhance operability. These involve assumptions in the calculation model, therefore, it’s essential to compare and validate the calculation results against temperature field monitoring data from actual ship operations. This approach provides crucial technical support for structural temperature field analysis.

REFERENCES

[1] Luo, M., Wang, X., Jin, X., Yan, B., 2020. Three-dimensional sloshing in a scaled membrane LNG tank under combined roll and pitch excitations. *Ocean Engineering*, 211, 1–10. https://doi.org/10.1016/j.oceaneng.2020.107578

[2] Nader, R., A., 2019. Environmental and cost-effectiveness comparison of dual fuel propulsion options for emissions reduction onboard LNG carriers. *Brodogradnja*, 70(3), 61–77. https://doi.org/10.21278/brod70304

[3] Tuswan, T., Sari, D. P., Muttaqie, T., Prabowo, A. R., Soetardjo, M., Murwantono, T. T. P., Utina, R., Yuniati, Y., 2023. Representative application of LNG-fuelled ships: a critical overview on potential GHG emission reductions and economic benefits. *Brodogradnja*, 74(1), 63–82. https://doi.org/10.21278/brod74104

[4] Andi, T., Haikal, A., Deddy, C., Samuel, S., 2022. Investigation of sloshing in the prismatic tank with vertical and T-shape baffles. *Brodogradnja*, 73(2), 43–57. https://doi.org/10.21278/brod73203

[5] Ahn, Y., Lee, J., Park, T., Kim, Y., 2023. Long-term approach for assessment of sloshing loads in LNG carrier, part II: Grouping method. *Marine Structures*, 89, 1–15. https://doi.org/10.1016/j.marstruc.2023.103398

[6] Zhang, W., Zhou, H., Cai, S., Chen, Y., Liu, C., 2008.Temperature field analysis of liquid cargo tank maintenance system of 138000m3LNG carrier. *China Shipbuilding*, 49(01): 77–83.

[7] Zhou, H., 2006. Study on convection coefficient of closed tank in LNG carrier. Beijing: Beijing University of Chemical Technology.

[8] Ding, S., 2010. Study on structural safety of large LNG ships under ultra-low temperature. Shanghai: Shanghai Jiao Tong University.

[9] Wu, J., He, J., Zhang, D., Lv, L., 2012. Study on temperature field analysis in membrane LNG carriers. Shipbuilding in China, 53(03), 75–84.

[10] Lv, L., 2013. Study on temperature field analysis of LNG ship. Shanghai: Shanghai Jiao Tong University.

[11] Lu, J., Xu, S., Deng, J., Wu, W., Wu, H., Yang, Z., 2016. Numerical prediction of temperature field for cargo containment system (CCS) of LNG carriers during pre-cooling operations. *Journal of Natural Gas Science and Engineering*, 29, 382–391. https://doi.org/10.1016/j.jngse.2016.01.009

[12] Wang, C., Qin, H., Shi, Z., Li, J., 2015. Research on calculation method of thermal field of large LNG-FSRU under ultra-low temperature. *Journal of Natural Gas Science and Engineering*, 33(3), 67–72. https://doi.org/10.18280/ijht.330309

[13] Li, G., Ju, Y., Fu, Y., 2015. Heat transfer model and evaporation rate calculation of new LNG ship liquid cargo insulation system. *Ship Engineering*, 37(03), 30–32.

[14] Wu, S., Jua, Y., Fu, Y., 2020. Numerical Study on Two-phase Flow and Phase Change Heat Transfer of Cryogenic Fluid in Type-B LNG Mock up Cargo Tank. *Journal of Refrigeration*, 41, 108–115.

[15] Wu, S., Jua, Y., Lina, J., Fu, Y., 2020. Numerical simulation and experiment verification of the static boil-off rate and temperature field for a new independent Type-B mock up tank in liquefied natural gas carrier. *Applied Thermal Engineering*, 173, 1–15. https://doi.org/10.1016/j.applthermaleng.2020.115265

[16] Niu, W., Li, G., Ju, Y., Fu, Y., 2017. Design and analysis of the thermal insulation system for a new independent type B LNG carrier. *Ocean Engineering*, 142, 51–61. https://doi.org/10.1016/j.oceaneng.2017.06.067

[17] China Classification Society, 2022. Code for Ship Construction and Equipment for Bulk Transport of Liquefied Gas (IGC Code). Beijing.

[18] U.S. Coast Guard, 2009. CFR46 part 154 Rules for foreign flag liquefied gas carriers intending to call at U.S. ports except ports in Alaska. USA.

[19] Yang, S., Tao, W., 2006. Heat Transfer. Beijing: Higher Education Press.